

# Effects of Noise, Magnitude Saturation, and Rate Limits on Rotating Stall Control

Yong Wang \*

yongwang@indra.caltech.edu

Richard M. Murray

murray@indra.caltech.edu

Division of Engineering and Applied Science  
California Institute of Technology  
Pasadena, California 91125

## Abstract

Operability enhancement is one of the major goals for active control of rotating stall and surge in axial compression systems. Using a reduced order model derived by Moore and Greitzer, we show that the operability enhancement achieved by bleed valve actuation is seriously limited by fluid noise, and actuator magnitude and rate limits. By approximating the attracting saddle-sink connections, we reduce the four dimensional model to a two dimensional system. Algebraic formulas relating the operability enhancement to the actuator limits, the fluid noise, and the shape of the compressor characteristic are obtained by approximating the stable manifold of a saddle fixed point for the reduced system. Finally, the reduction and approximation techniques are shown to be viable by numerical simulations for a model of a low speed rig with a fast valve and a slow valve.

## 1. Introduction

Aeroengine performance is limited by two aerodynamic instabilities in the compression system called rotating stall and surge. Rotating stall occurs when a nonaxisymmetric flow disturbance develops around the annulus of the rotor and causes drastic reduction in the performance of the compressor. Once rotating stall develops, the compressor cannot recover back to steady axisymmetric flow condition due to the hysteresis. Rotating stall may also induce large amplitude axisymmetric oscillations across the compression system called surge. Rotating stall stabilization refers to control laws that achieve operability enhancement, which means extension of the stable axisymmetric operating range, or elimination of the hysteresis at the stall inception point. Experimentally there are essentially three basic types

of active actuators that have been used for active stall stabilization, namely inlet guide vanes (IGVs) (see [10]), air injectors (see [3, 5, 2]) and outlet bleed valves (see [1, 4]).

On the theoretical end, the design and analysis of controllers for rotating stall and surge stabilization are based on the model derived by Moore and Greitzer in their seminal paper [9]. An important implication of the Moore Greitzer model is that the precursors to rotating stall are disturbances in the form of traveling waves around the annulus of the compressor. The three state Moore Greitzer model is the Galerkin projection of the PDEs to the zeroth (axisymmetric) and the first spatial harmonics. One of the attractive features of the three state Moore Greitzer model is that it captures the main dynamical behavior of both surge and rotating stall, and is simple enough for designing active controllers (see [7, 8]). Although many bleed valve controllers have been designed using Lyapunov stability theory and dynamical system theory, few have addressed the effects of actuator limitations and fluid noise. In [6], gain and phase margin of different controllers based on the linearized Moore Greitzer model are used to evaluate the effectiveness of different actuations.

In this paper we consider the following problem: Given a low  $B$  three state model for an axial compression system and a bleed valve actuator with magnitude saturation and rate limits, how much operability enhancement can be achieved? Due to the magnitude and rate saturation of the controller as well as the strong nonlinearity of the three state Moore Greitzer model around the stall inception point, tools in linear control theory may not be applicable to the above problem. Although the operability enhancement can be obtained by numerical simulations of the full system, the functional relations between the operability enhancement and the actuator

---

\*Funding for this research was by AFOSR grant F49620-95-1-0409.

limits, fluid noise and compressor parameters may not be easy to see from numerical simulations. In this paper, we develop a framework to analyze the effects of actuator limits via nonlinear reduction of the three state Moore Greitzer model. From this framework, approximate analytical formulas could be obtained which have shown good agreement with the results from simulations to a high fidelity model as well as experiments for a low speed compressor (see [12]).

The framework is as follows. First, due to the fact that for small  $B$  parameter, neither classic surge nor deep surge occurs for the three state Moore Greitzer model with a cubic compressor characteristic (see [8]), we approximate the dynamics on the attracting saddle-sink connections by a one dimensional system, which together with the one dimensional ordinary differential equation describing the dynamics of the controller, forms a two dimensional dynamical system. Secondly, the effects of actuator limits and fluid noise on the operability enhancement are derived by studying this two dimensional dynamical system using the approach of phase plane analysis. Finally, we illustrate the theoretical results by considering the three state Moore Greitzer model for an experimental rig at Caltech with a fast bleed valve and a slow bleed valve.

## 2. Background and motivation

The three state Moore Greitzer model for axial compression systems is as follows [9]:

$$\begin{aligned} \frac{d\Phi}{d\xi} &= \frac{1}{l_c} \left( \frac{1}{2\pi} \int_0^{2\pi} \psi_c(\Phi + A \sin \zeta) d\zeta - \Psi \right), \\ \frac{d\Psi}{d\xi} &= \frac{1}{4B^2 l_c} (\Phi - \Phi_T(\Psi)), \\ \frac{dA}{d\xi} &= \frac{1}{\pi} \frac{1}{m + \mu} \int_0^{2\pi} \psi_c(\Phi + A \sin \zeta) \sin \zeta d\zeta, \end{aligned} \quad (1)$$

where  $\Phi$  is the annulus-averaged axial flow coefficient,  $\Psi$  is the annulus-averaged total-to-static pressure rise coefficient,  $A$  is the amplitude of the first harmonic of the axial flow disturbances around the compressor annulus,  $\psi_c(\cdot)$  is the compressor characteristic,  $\Phi_T(\cdot)$  is the throttle characteristic,  $l_c$  is the effective length of the compression system,  $B$  is the Greitzer  $B$ -parameter,  $m$  is the duct parameter,  $\mu$  is the inertia parameter,  $\xi$  is the nondimensional time,  $\zeta$  is the circumferential angle around the compressor annulus. Suppose the compressor characteristic is analytic and the throttle characteristic is  $\Phi_T(\Psi) = (\gamma + u)\sqrt{\Psi}$ , where  $u$  is the control input of the bleed valve and  $\gamma$  is the throttle coefficient denoting the opening of the throttle ( $\gamma = 0$  means

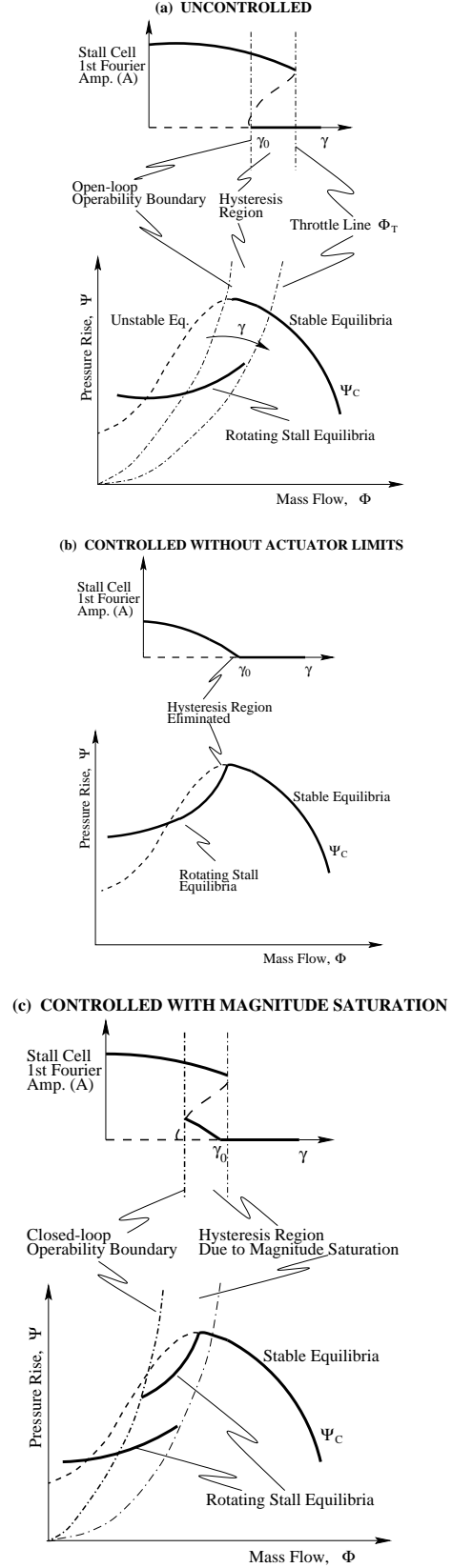


Figure 1: Effects of bleed valve controllers

the throttle is fully closed). In the following we only consider the feedback control law by Liaw and Abed [7] with first order actuator dynamics and magnitude and rate saturations given by

$$\frac{du}{d\xi} = \begin{cases} \frac{u_{des} - u}{\tau} & \text{if } \frac{u_{des} - u}{\tau} < u_{rate}, \\ u_{rate} & \text{if } \frac{u_{des} - u}{\tau} \geq u_{rate}, \end{cases} \quad (2)$$

$$u_{des} = \begin{cases} KJ & \text{if } KJ < u_{mag}, \\ u_{mag} & \text{if } KJ \geq u_{mag}. \end{cases}$$

Suppose  $B$  is sufficiently small such that there is no Hopf bifurcation to surge for the three state Moore Greitzer model. Figure 1 shows the typical performance of the open loop and the closed loop system for the Liaw-Abed control law (Figure 1(a) and (b) are from J. D. Paduano). Figure 1(a) shows the behavior of the uncontrolled system. The operating point of the compressor is the intersection of the compressor characteristic  $\psi_c$  and the throttle characteristic  $\Phi_T$ . Physically this operating point denotes the steady axisymmetric flow condition. This operating point becomes unstable when the slope of  $\psi_c$  becomes positive, and the dynamics converges to a new “stalled” equilibrium, which denotes the unsteady nonaxisymmetric flow pattern rotating around the rotor face at about a half of the rotor speed. This stalled equilibrium has an associated hysteresis effect, whereby opening the throttle does not return the system to the original operating point. This hysteresis effect can also be seen in the upper plot of Figure 1(a). Figure 1(b) illustrates the behavior of the controlled system (1) with Liaw-Abed control law  $u = KJ$ , i.e., there are no actuator limitations. The effect of the Liaw-Abed control law is to eliminate the hysteresis. This allows significant benefit in operability since the system can be operated more closely to the peak of the compressor characteristic.

In fact, however, no physical controller has infinite magnitude saturation limit and infinite bandwidth. For the active control of rotating stall, the actuator limits play a particularly important role. One reason is that the growth time of the stall cell can be very short. For instance, for the Caltech rig described in Section 5, the time for stall cell formation is about 0.03 second at the stall inception point (see [2]). Another reason is that the magnitude saturation for the bleed valve is unavoidable since in practice it is undesirable to bleed more than twenty percent of the flow through the compressor. Now suppose the magnitude saturation for the Liaw-Abed controller is finite but the actuator bandwidth is infinite, i.e., the valve is infinitely fast but it can only

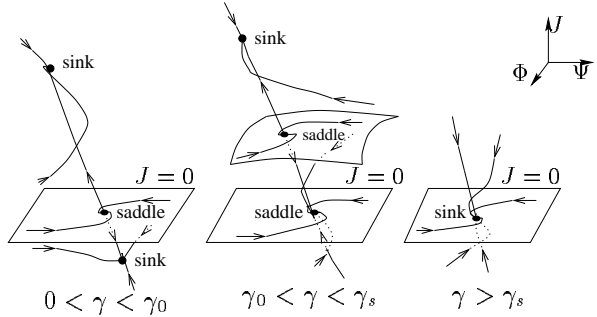


Figure 2: Phase portraits for the three state Moore Greitzer model at different throttle coefficients.

bleed out a certain amount of air. The bifurcation diagram for the closed loop system (1) and (2) is shown in Figure 1(c). It can be seen that there is a hysteresis loop due to magnitude saturation of the bleed valve. This hysteresis loop defines the operability boundary for the closed loop system. We define the operability enhancement as the gap between the open loop operability boundary and the closed loop operability boundary. If the bleed valve is not infinitely fast, then the operability enhancement is further restrained by the rate limits. The goal of the following sections is to evaluate the operability enhancement.

### 3. Reduction

We assume the qualitative phase portraits of the open loop system for different  $\gamma$ 's look like Figure 2. Let  $\Phi_0$ ,  $\Psi_0$  and  $\gamma_0$  be the axial flow coefficient, the pressure rise coefficient, and throttle coefficient at the peak of the compressor characteristic, respectively. Let  $\gamma_s$  be the throttle coefficient at which the unstable stall equilibria merge with the stable stall equilibria. The following proposition gives the center manifold reduction of the uncontrolled system.

**Proposition 1** *For sufficiently small  $B$ , the dynamics of (1) near the transcritical bifurcation point  $(\Phi_0, \Psi_0, 0)$  can be approximated by the dynamics on the center manifold and can be approximated by the following ordinary differential equation*

$$\frac{dJ}{d\xi} = \alpha_1(\delta + u)J + \alpha_2 J^2 + \mathcal{O}((\delta + u)J^2, J^3), \quad (3)$$

where  $J = A^2$ ,  $\delta = \gamma - \gamma_0$ ,

$$\alpha_1 = \frac{2\sqrt{\Psi_0}\psi_c''}{m + \mu}, \quad (4)$$

$$\alpha_2 = \frac{1}{4(m + \mu)} \left( \psi_c''' + \frac{\gamma_0 \psi_c''^2}{\sqrt{\Psi_0}} \right), \quad (5)$$

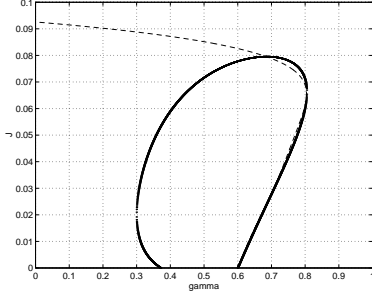


Figure 3: The stall equilibria of the MG3 and the approximate 1D system for the Caltech rig, solid line: MG3, dashed line: reduced 1D system.

and all the derivatives of  $\psi_c$  are evaluated at  $\Phi_0$ .

The proof of Proposition 1 is the standard center manifold reduction of the full model (1) (see [11]). The coefficients in the center manifold equation determine the bifurcation characteristics of the full three state Moore Greitzer model in the neighborhood of  $\gamma_0$ . For a typical compressor characteristic, the second derivative at the peak is negative, so  $\alpha_1 < 0$ . If  $\alpha_2 > 0$ , then the transcritical bifurcation to rotating stall is subcritical; if  $\alpha_2 < 0$ , then the transcritical bifurcation to rotating stall is supercritical. The subcritical bifurcation is more detrimental in that small disturbances will grow to large amplitude stall cells. The Liaw-Abed feedback control law  $u = KJ$  makes the closed loop system be supercritical if  $K > -\alpha_2/\alpha_1$ .

We use the following system to approximate the dynamics on the attracting saddle-sink connections (see Figure 2):

$$\dot{J} = \alpha J \left( \alpha_1(\gamma - \gamma_0 + u) + \sum_{k=2}^n \alpha_k J^{k-1} \right), \quad (6)$$

where  $u$  is the control input whose dynamics is given by (2), and the  $\alpha$ 's are selected such that the equilibria of the ordinary differential equation (6) fit the projection of the equilibria of the full system to the  $\gamma$ - $J$  plane in the following way:

- 1)  $\alpha_1$  and  $\alpha_2$  are taken from the center manifold equation (4) and (5).
- 2)  $\alpha_k$  ( $k = 3, \dots, n$ ) are selected such that the equilibria of the one dimensional system (6) fit the equilibria of the full system in the hysteresis region.

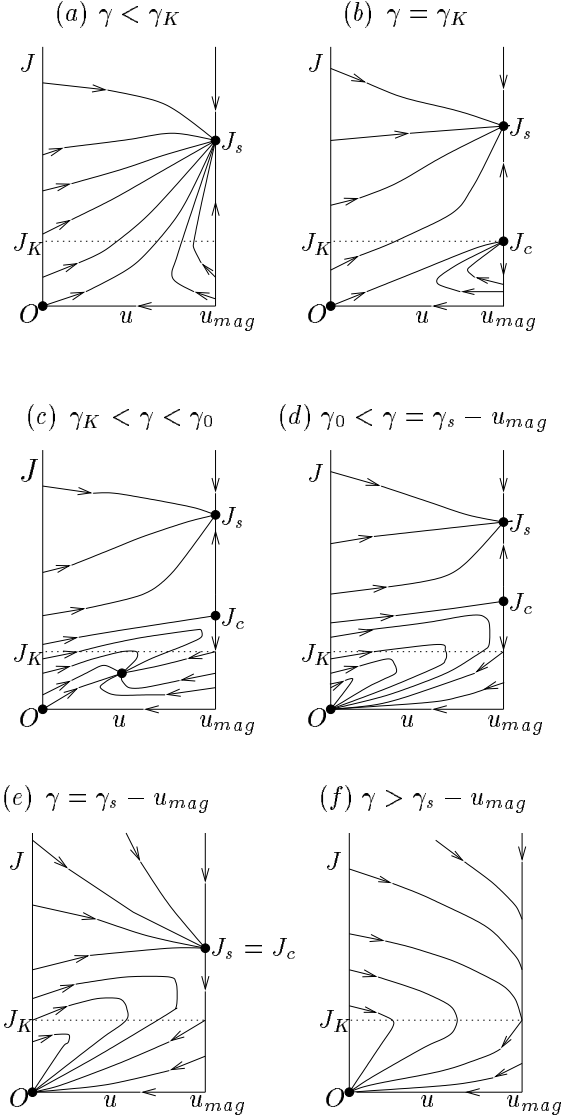


Figure 4: Phase portraits for different throttle operating positions.

- 3)  $\alpha$  is selected such that the growth rate of  $J$  for the approximate system (6) matches that for the full system at  $\gamma = \gamma_0$ .

Figure 3 show the stall equilibria for the three state Moore Greitzer model for the Caltech rig with a fourth order polynomial compressor characteristic and the stall equilibria for the reduced system with  $n = 7$ .

Due to the magnitude saturation and the rate limits, different regions in the  $u$ - $J$  phase plane are governed by different control laws. Let

$$\gamma_K = \gamma_0 - u_{mag} - \frac{\alpha_2 u_{mag}}{\alpha_1 K}, \quad J_K = \frac{u_{mag}}{K}.$$

Assuming  $u_{mag} < \gamma_s - \gamma_0$ , the qualitative phase portraits for the reduced two dimensional system (6) and (2) at different operating throttle positions are shown in Figure 4. Figure 4(a) shows that if the throttle is operated at a throttle position  $\gamma$  such that  $\gamma < \gamma_K$ , then all the flows except  $J = 0$  converge to the fully developed rotating stall and actuator magnitude saturation equilibrium  $(u_{mag}, J_s)$ , i.e., any small noise of  $J$  will evolve to the fully developed rotating stall. Hence  $\gamma_K$  defines the closed loop operability boundary for infinitely small noise (initial conditions of  $J$ ). Figure 4(b) shows that if the throttle is operated at  $\gamma$  such that  $\gamma = \gamma_K$ , then some trajectories converge to the saddle  $(u_{mag}, J_c)$ , while others converge to  $(u_{mag}, J_s)$ . Figure 4(c) shows that if the throttle is operated at  $\gamma$  such that  $\gamma_K < \gamma < \gamma_0$ , then there two different regions in the  $u$ - $J$  plane divided by the stable manifold of the saddle: the trajectories above the stable manifold converge to the fully developed rotating stall equilibrium, the trajectories below the stable manifold converge to the stabilized rotating stall equilibrium. Figure 4(d) shows that if the throttle is operated at  $\gamma$  such that  $\gamma_0 < \gamma < \gamma_s$ , then the trajectories below the stable manifold of the saddle converge to the axisymmetric equilibrium  $(0, 0)$ . Figure 4(e) shows that if the throttle is operated at  $\gamma$  such that  $\gamma = \gamma_s$ , then some trajectories converge to the saddle, while others approach the stable axisymmetric equilibrium  $(0, 0)$ . Figure 4(f) shows that if the throttle is operated at  $\gamma$  such that  $\gamma > \gamma_s$ , then  $(0, 0)$  is globally stable.

If  $u_{mag} > \gamma_s - \gamma_0$ , then the phase portrait Figure 4(c) is valid for  $\gamma$  such that  $\gamma_K < \gamma < \gamma_s - u_{mag}$  and the phase portrait Figure 4(d) valid for  $\gamma$  such that  $\gamma_s - u_{mag} < \gamma < \gamma_s$ , while the rest are the same as the case when  $u_{mag} < \gamma_s - \gamma_0$ .

#### 4. Analysis

In this section we give the approximate algebraic relations from which the closed loop operability boundary is as a function of the actuator limits and the shape of the compressor characteristic.

From Figure 4(c), we know that the stable manifold of the saddle fixed point in the  $u$ - $J$  plane divides the phase plane into two regions: one region contains all the trajectories converging to the fully developed rotating stall equilibrium, the other region contains all the trajectories converging to the stabilized rotating stall equilibrium. The intersection of the stable manifold of the saddle fixed point and the line  $u = 0$  is the boundary of initial conditions of  $J$  from which the trajectories will converge to the stabilized rotat-

ing stall equilibrium. By a first order approximation to the stable manifold of the saddle, we could obtain algebraic relations from which the closed loop operability boundary may be solved as all other parameters. Let  $\delta = \gamma - \gamma_0$  be the operability enhancement. If  $\tau u_{rate} \geq u_{mag}$ , then  $\delta$  as a function of other parameters is given by the following algebraic equations

$$\begin{aligned} \epsilon &= \frac{1}{K} (u_{mag})^{\frac{1}{1+\tau\alpha\alpha_1\delta}} \cdot \\ &\quad (-\tau\alpha\alpha_1\delta u_{mag} - x_c(1 + \tau\alpha\alpha_1\delta))^{\frac{\tau\alpha\alpha_1\delta}{1+\tau\alpha\alpha_1\delta}}, \\ x_c &= \left( \frac{1}{\alpha\alpha_1\tau} - \delta - u_{mag} \right) \left( 1 + \frac{\alpha_2 u_{mag}}{K\alpha_1(\delta + u_{mag})} \right), \end{aligned}$$

where  $\epsilon$  denotes the noise level which is defined as the largest initial conditions for  $J$ . The case when  $\tau u_{rate} \leq u_{mag}$  can be analyzed similarly, though it is more complicated.

Now we consider an extreme case, namely,  $K = +\infty$ ,  $\tau = 0$ . Physically this means the following open loop control algorithm: as soon as the sensors detect that the stall cell has grown out of the fluid noise level at time  $\xi = 0$ , the bleed valve is driven to open as fast as possible to catch the stall cell until the valve saturates in magnitude. Experiments have shown that when implementing this control algorithm, there are also such time delays as valve mechanical delay, delay caused by the compressibility of air and delay caused by the filter. These time delays are not negligible and seriously affect the operability enhancement. By taking account of all these delays, we use the following actuator dynamics for  $J(0) > J_{thresh} \geq \epsilon$  ( $J_{thresh}$  is the threshold):

$$u = \begin{cases} 0 & \text{if } 0 \leq \xi < \xi_1, \\ u_{rate}(\xi - \xi_1) & \text{if } \xi_1 \leq \xi < \xi_2, \\ u_{rate}(\xi_2 - \xi_1) & \text{if } \xi \geq \xi_2, \end{cases} \quad (7)$$

otherwise if  $J(0) \leq J_{thresh}$ , then  $u = 0$ . Here  $J(0)$  is the value of  $J$  at  $\xi = 0$ , and  $\xi_1$  is the sum of all the time delays. Instead of analyzing the full model (1) and (7), we consider the two dimensional reduced system (6) and (7). Figure 5 shows the qualitative phase portrait of this two dimensional system. By approximating the stable manifold of the saddle, we get the following algebraic equations

$$\begin{aligned} J_c &= J_1 e^{\alpha(\alpha_1\delta + \lambda(J_1))\xi_1}, \\ J_1 &= J_{crit} e^{\alpha(\alpha_1\delta + \lambda(J_{crit}))\xi_1}, \\ J_c &= -\frac{\alpha_1}{\alpha_2}(\delta + u_{mag}), \end{aligned} \quad (8)$$

where  $u_{mag} = u_{rate}(\xi_2 - \xi_1)$ , and

$$\lambda(x) = \sum_{k=2}^n k\alpha_k x^{k-1}.$$

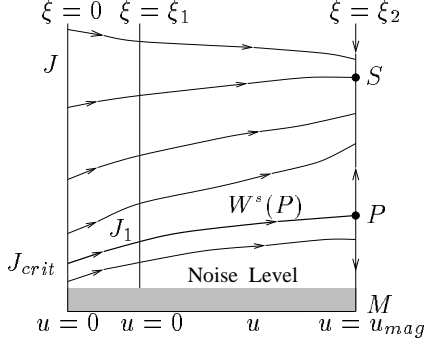


Figure 5: Phase portrait for the reduced system (6) and (7).

Suppose the noise level is  $\epsilon$ . Letting  $J_{crit} = \epsilon$ , then from above algebraic equations the closed loop operability boundary  $\delta_{crit}(\xi_1, \xi_2)$  may be solved. Define the nondimensional operability enhancement as

$$\eta_\gamma(\xi_1, \xi_2) = \frac{\hat{\gamma} - (\gamma_0 + \delta_{crit}(\xi_1, \xi_2))}{\hat{\gamma}},$$

where  $\hat{\gamma}$  is uncontrolled system operability boundary for the noise level  $\epsilon$ . We also call  $\eta_\gamma(\xi_1, \xi_2)$  the extension of stable region since all trajectories from the noise level converge to the axisymmetric operating point. By calculating the axisymmetric flow rate  $\Phi_{crit}$  corresponding to the critical throttle coefficient  $\gamma_{crit} := \gamma_0 + \delta_{crit}$ , we get the extension of stable operating region in terms of flow coefficient

$$\eta_\Phi(\xi_1, \xi_2) = \frac{\hat{\Phi} - \Phi_{crit}(\xi_1, \xi_2)}{\hat{\Phi}},$$

where  $\hat{\Phi}$  is the axial flow coefficient when the throttle coefficient is  $\hat{\gamma}$ .

## 5. Examples

In this section, we apply the ideas in previous sections to two examples: the Caltech rig with a slow valve and a fast valve. The experimental setup for the Caltech compressor is described in [2]. The description for the fast bleed valve and the slow valve is in [12]. Here we use a fourth order polynomial to fit the more precise piecewise continuous compressor characteristic for the Caltech rig, i.e.,

$$\psi_c(\Phi) = a_1\Phi^4 + a_2\Phi^3 + a_3\Phi^2 + a_4\Phi + a_5,$$

where the coefficients and parameters are

$$\begin{aligned} a_1 &= 61.6, & a_2 &= -93.8, & a_3 &= 44.5, \\ a_4 &= -6.85, & a_5 &= 0.426, & l_c &= 1.3, \\ m + \mu &= 0.7, & B &= 0.2. \end{aligned}$$

Rig/Bleed	Method	$\eta_\gamma$	$\eta_\Phi$
Fast Valve (12% bleed)	MG3 (Simulation)	1.4 %	1.4 %
	2D Appr. Syst. (Simulation)	1.6 %	1.6 %
	2D Appr. Syst. (Appr. Stable. Mfld)	1.3 %	1.3 %
Slow Valve (15% bleed)	MG3 (Simulation)	0.4 %	0.4 %
	2D Appr. Syst. (Simulation)	0.5 %	0.5 %
	2D Appr. Syst. (Appr. Stable. Mfld)	0.07 %	0.07 %

Figure 6: Comparison of different methods for evaluation of the operability enhancement.

By the procedure in Section 3, we use the two dimensional system (6) and (7) to approximate the dynamics on the attracting saddle-sink connections of the full system (1) and (7). The parameters are as follows.

$$\begin{aligned} \gamma_0 &= 0.599, & \alpha &= 1.3, \\ \alpha_1 &= -22.4, & \alpha_2 &= 75.2, \\ \alpha_3 &= -1.05 \times 10^3, & \alpha_4 &= 1.40 \times 10^5, \\ \alpha_5 &= -5.43 \times 10^6, & \alpha_6 &= 8.56 \times 10^7, \\ \alpha_7 &= -4.86 \times 10^8, & \epsilon &= 7.8 \times 10^{-4}. \end{aligned}$$

for the fast valve

$$\begin{aligned} \xi'_1 &= 1.7, & \xi'_2 &= 3.9, & \nu &= 0.12, \\ u_{mag} &= 0.072, & u_{rate} &= 0.033, \end{aligned}$$

for the slow valve

$$\begin{aligned} \xi'_1 &= 3.14, & \xi'_2 &= 12.6, & \nu &= 0.15, \\ u_{mag} &= 0.090, & u_{rate} &= 0.009. \end{aligned}$$

To obtain the extension of stable region, we have simulated the full fourth order model (1) and (7), where the initial conditions for  $\Phi$  and  $\Psi$  are the axisymmetric equilibrium for each  $\gamma$ , the initial condition for  $J$  is  $\epsilon$ , and the initial condition for  $u$  is 0. We have also simulated the two dimensional approximate system (6) and (7) with initial conditions for  $J$  and  $u$  being  $\epsilon$  and 0. We have also computed the extension of stable region using formulas (8). In summary, the results for the estimates of the extended stable operating region are shown in Figure 6. From these results it can be seen that the approximation procedure in the above sections gives good approximation of full system.

Due to the noise and step size of varying the disturbance throttle, it is estimated that the extension of stable region can be observed in the Caltech rig only if the extension of stable region is greater than

3 percent. Experiments have shown that no extension of stable region has been achieved by the two valves, i.e., stall inception point for the controlled system is the same as the that for the uncontrolled system. From (8) it can be seen that the extension of stable region is a function of  $\alpha_1$  and  $\alpha_2$ , which are determined by the shape of the compressor characteristic and other compressor parameters. It have shown in [12] that extension of stable region has been achieved experimentally on the Caltech rig using the fast bleed valve together with continuous air injection, whereby the continuous air injection changes the shape of the compressor characteristic and reduced the rate requirement for stall control. The framework in this paper have been applied to this case and have shown good agreement with the experimental results (see [12]).

## 6. Summary

In this paper, we have given a general framework for analyzing the effects of actuator limitations for bleed valve controllers on rotating stall control. The main assumption is that the Greitzer  $B$  parameter is small such that the saddle-sink connections are attracting, so that we could use the center manifold reduction to the full system. The effects of actuator limitations and fluid noise are obtained via phase plane analysis of the reduced system. Numerical simulations have shown that the formulas derived from the reduced system given good approximation of the full three state Moore Greitzer model for the Caltech rig with a slow valve and a fast valve. Our analysis has shown that high bandwidth bleed valve actuators are highly desirable in order to enhance the operability of a compression system.

**Acknowledgments** The authors would like to thank R. L. Behnken, S. Yeung, B. D. Collier and R. D’Andrea for many useful discussions. The experiments done by Yeung and Behnken using the bleed valve actuators to control the rotating stall in the Caltech rig are the source of the motivation.

## References

- [1] Badmus, O. O., Chowdhury, S., Eveker, K. M., Nett, C. N., and Rivera, C. J., 1993, “A Simplified Approach for Control of Rotating Stall—Part 2: Experimental Results”, *29th Joint Propulsion Conference and Exhibit, AIAA Paper #93-2234*.
- [2] D’Andrea, R., Behnken, R. L., and Murray, R. M., 1995, “Active Control of Rotating Stall Using Pulsed Air Injection: Experimental Results on a Low-Speed Axial Flow Compressor”, *Sensing, Actuation, and Control in Aeropropulsion*, J. D. Paduano, Editor, Proc. SPIE 2494, pp. 152-165.
- [3] Day, I. J., 1993, “Active Suppression of Rotating Stall and Surge in Axial Compressors”, *ASME Journal of Turbomachinery*, Vol. 115, pp. 40-47.
- [4] Eveker, K. M., Gysling, D. L., Nett, C. N., and Sharma, O. P., 1995, “Integrated Control of Rotating Stall and Surge in Aeroengines”, *Sensing, Actuation, and Control in Aeropropulsion*, J. D. Paduano, Editor, Proc. SPIE 2494, pp. 21-35.
- [5] Gysling, D. L., and Greitzer, E. M., 1994, “Dynamic Control of Rotating Stall in Axial Flow Compressor Using Aeromechanical Feedback”, *ASME Journal of Turbomachinery*, Vol. 117, No. 3, pp. 307-319.
- [6] Hendricks, G. J., and Gysling, P. L., 1994, “Theoretical Study of Sensor-Actuator Schemes for Rotating Stall Control”, *Journal of Propulsion and Power*, Vol. 10, No. 1, pp. 101-109.
- [7] Liaw, D. C., and Abed, E. H., 1996, “Control of Compressor Stall Inception: A Bifurcation-Theoretic Approach”, *Automatica*, Vol. 32, No. 1, pp. 109-115.
- [8] McCaughan, F. E., 1990, “Bifurcation Analysis of Axial Flow Compressor Stability”, *SIAM J. Appl. Math.*, Vol. 50, No. 5, pp. 1232-1253.
- [9] Moore, F. K., and Greitzer, E. M., 1986a, “A Theory of Post-Stall Transients in Axial Compression Systems: Part I—Development of Equations”, *ASME Journal of Engineering for Gas Turbines and Power*, Vol. 108, pp. 68-76.
- [10] Paduano, J. D., Epstein, A. H., Valavani, L., Longley, J. P., Greitzer, E. M., and Guenette, G. R., 1993, “Active Control of Rotating Stall in a Low-Speed Axial Compressor”, *ASME Journal of Turbomachinery*, Vol. 115, pp. 48-56.
- [11] Wiggins, S., Introduction to Applied Nonlinear Dynamical Systems and Chaos, *Springer-Verlag*, 1990.
- [12] Yeung, S., and Murray, R. M., Reduction of Bleed Valve Rate Requirements for Control of Rotating Stall using Continuous Air Injection (to appear in *Proceedings of 6th IEEE Conference on Control Applications*, 1997.)